Available online at www.sciencedirect.com
SCIENCE DIRECT®
ELSEVIER
Dyes and Pigments 69 (2006) 118–127
DYES and PIGMENTS
www.elsevier.com/locate/dyepig

Symmetrical and unsymmetrical perylene diimides: Their synthesis, photophysical and electrochemical properties

Nur Pasaogullari [a], Huriye Icil [a,*], Martin Demuth [b]

[a] *Department of Chemistry, Faculty of Arts and Science, Eastern Mediterranean University, Famagusta, N. Cyprus, Mersin 10, Turkey*
[b] *Max Planck Institute for Bioinorganic Chemistry, D-45413 Muelheim an der Ruhr, Germany*

Received 12 November 2004; received in revised form 3 March 2005; accepted 4 March 2005

Abstract

New unsymmetrical perylene diimides have been synthesized to investigate their potential for applications. The symmetrical derivatives of all the compounds have been synthesized for comparison. The compounds are characterized by UV–vis, IR, MS, DSC, TGA and CV measurements. The fluorescence lifetimes, quantum yields and singlet-state energies are presented. All the compounds have very similar fluorescence lifetimes. The LUMO energy values of all the compounds as determined by cyclic voltammetry, are nearly identical. *N*-substituents have little influence on the electrochemical behavior of all the compounds. The color, solubility, thermal stability, extinction coefficients, aggregation and fluorescence quantum yields are dependent on the nature of the *N*-substituents. They show different aggregation in solid state.

Keywords: Perylenes; Fluorescence dyes; Unsymmetrical pigments; Aggregation

1. Introduction

Perylene diimides have been extensively studied due to their high molar absorptivity, high quantum yields of fluorescence with excellent photochemical and thermal stability [1–6]. They have been used in photovoltaic devices [7], solar cells [8] and dye lasers [9]. Symmetrical perylene diimides could be synthesized easily in high yield by reactive primary amines in *m*-cresol and isoquinoline [1–6].

The synthesis of unsymmetrical perylene diimides has been described by Nagao and Misono [10–13], Tröster [14] and Langhals [1,15–17] with good yields. The control of the self-organisation of dye molecules in solution by bulky peripheral groups has been demonstrated by Langhals et al. [15]. *N*-octadecyl-3,4,9,10-perylenetetracarboxylic monoanhydride monoimide with a low quantum yield was specially synthesized for the study of the electromagnetically surface-enhanced fluorescence by Aroca [18]. Spectroscopic characterization of some Langmuir–Blodgett film forming symmetrical or unsymmetrical perylene diimides has been reported by Aroca [19]. Zhavnerko et al. have reported the structure and properties of monomolecular films based on *N*-octadecyl-3,4,9,10-perylene-bis(dicarboxydiimide) [20]. The investigation and development of new symmetrical and unsymmetrical perylene dyes are important to broaden our understanding of sensitizing materials in general.

In previous papers, the synthesis of symmetrical perylene dyes (**1a–f**) [2–6], 3,4,9,10-perylenetetracarboxylic-3,4-anhydride-9,10-imide (**3a**) [14] and *N*-dodecyl-3,4,9,10-perylenebis(dicarboximide) (**4a**) has been described [19]. The purpose of this work was to

---

* Corresponding author. Tel.: +90 392 630 1085; fax: +90 392 630 2545.
E-mail address: huriye.icil@emu.edu.tr (H. Icil).

0143-7208/$ - see front matter © 2005 Elsevier Ltd. All rights reserved.
doi:10.1016/j.dyepig.2005.03.001

synthesize some novel perylene compounds: a new perylene monoimide *N*-(4-hydroxyphenyl)-3,4,9,10-perylenetetracarboxylic-3,4-anhydride-9,10-imide (**3b**), new unsymmetrical perylene dyes **4b**, **4c**, **4d**, **4e**, **4f** as the monosubstituted perylene diimides and **4g**, **4h** having different substituents on *N* and *N′* atoms. The structure of all the compounds was checked by IR, ^{1}H NMR, UV–vis, MS and elemental analysis. Meanwhile, NMR analysis of the unsymmetrical perylene dyes could not be taken due to the very poor solubility.

In this article we describe the synthesis of two types of perylenes: first, the synthesis of symmetrical perylene diimides (Fig. 1, **1a–f**) by the condensation of perylene dianhydride with corresponding amines [2–6] and secondly, the synthesis of unsymmetrical perylenebis-(dicarboximide) derivatives (Fig. 1, **4a–h**) by the condensation of *N*-alkyl-3,4,9,10-perylenetetracarboxylic monoanhydride (Fig. 1, **3a**, **b**) with the same amines.

The optical, photochemical, thermal and electrochemical properties of symmetrical and unsymmetrical perylene diimides have been investigated in detail.

2. Experimental

2.1. Chemicals and instruments

Perylene-3,4,9,10-tetracarboxylic dianhydride, dodecylamine, 1,12-diaminododecane, octadecylamine, *p*-phenylenediamine, 4-chloroaniline, 4-aminophenol, potassium hydroxide, potassium carbonate, ammonia solution 25%, isoquinoline and *m*-cresol were obtained from Aldrich. Tetrabutylammonium hexafluorophosphate (TBAPF6) and ferrocene were used as received from Fluka. All organic solvents employed were of spectroscopic grade.

IR spectra were measured as KBr pellets using a Brucker IFS 66 spectrometer. UV spectra in solutions were recorded with a Varian-Cary 100 spectrometer. UV spectra of solid state were measured in thin films using a Perkin–Elmer UV/VIS/NIR Lambda 19 spectrometer, equipped with solid accessories. Mass spectra were recorded with a Finnigan MAT 311A instrument at 70 eV ionization energy. Data were presented in *m*/*z* (%) values. Emission spectra were measured using a Spex fluorolog. Elemental analyses were obtained from a Carlo-Erba-1106 C, H, N analyzer. TGA thermograms were recorded with a TG–MS: Simultane TG-DTA/DSC apparatus STA 449 Jupiter from Netzsch, equipped with Balzers Quadstar 422 V. The samples were heated at 5 K/min in oxygen. Thermal analyses were recorded using a DSC 820 Mettler Toledo instrument. The samples were heated at 5 K/min in nitrogen. Cyclic and square-wave voltammetries in butyronitrile were performed using a three-electrode cell with a polished 2 mm glassy carbon as working and Pt as counter electrode; solutions were 10^{-4} M in electroactive material and 0.1 M in supporting electrolyte, tetrabutylammonium hexafluorophosphate (TBAPF6). Data were recorded on an EG & G PAR 273A computer-controlled potentiostat. Ferrocene was used as an internal reference. The scan rate of 100–400 mV s^{-1} and the frequency 60 Hz were employed for cyclic and square-wave voltammetries, respectively. Fluorescence lifetime measurements were performed by time correlated single photon counting technique (FLS920, from Edinburgh Instruments).

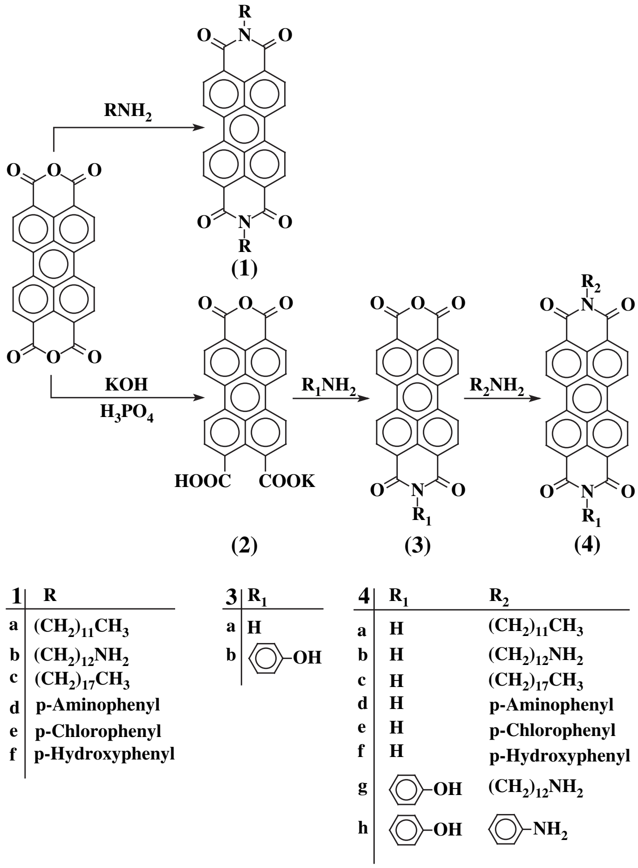

Fig. 1. Synthesis of symmetrical (**1a–f**) and unsymmetrical (**4a–h**) perylene diimides.

2.2. Representative preparation of unsymmetrical 3,4,9,10-perylenebis(dicarboximide) derivatives (4a–h)

Symmetrical 3,4,9,10-perylenebis(dicarboximide) derivatives (**1a–f**) were synthesized as previously described [2–6].

Compounds (**4a–h**) were synthesized by the method previously reported [14]. Unsymmetrical perylene dyes were prepared via a three-step reaction. At the first step, perylene-3,4,9,10-tetracarboxylic acid monoanhydride monopotassium carboxylate (**2**) was synthesized according to literature [13]. At the second step, *N*-alkyl(aryl)-3,4,9,10-perylene tetracarboxylic monoanhydride monoimide was prepared (**3a–b**) [14]. Finally, the unsymmetrical perylene dyes (**4a–h**) were synthesized via condensation of corresponding amines with the *N*-alkyl(aryl)-3,4,9,10-perylene tetracarboxylic monoanhydride monoimide (**3a**, **b**) using *m*-cresol and isoquinoline as solvent mixture [1–6].

2.3. Perylene-3,4,9,10-tetracarboxylic acid monoanhydride monopotassium carboxylate (2)

Perylene-3,4,9,10-tetracarboxylic acid dianhydride (3 g, 7.6 mmol) was stirred in KOH solution (5%, 35 mL) for 4 h at 90 °C. After cooling to room temperature, 12.5 mL H_3PO_4 (10%) was added and stirred for 1 h at 90 °C. The precipitate formed was filtered, washed with water and dried in vacuum at 100 °C.

2: Yield 89% (3.1 g, bordeaux-red powder). FT-IR (KBr, cm^{-1}): ν = 3437, 3065, 2460, 1935, 1770, 1727, 1593, 1508, 1407, 1376, 1342, 1315, 1302, 1232, 1211, 1183, 1151, 1122, 1017, 939, 854, 818, 809, 766, 740, 687,641, 612, 536, 499, 485, 463, 450, 436, 442, 415. UV/vis (DMF): λ_{max} (nm) (ε) = 453 (11 400), 481 (26 000), 518 (37 800). Anal. Calcd. for $C_{24}H_9KO_7$ (M_w, 448.4); C, 64.28; H, 2.02; K, 8.72. Found: C, 63.8; H, 2.1; K, 8.6.

2.4. N-alkyl(aryl)-3,4,9,10-perylene tetracarboxylic monoanhydride monoimide (3a, b)

Perylene-3,4,9,10-tetracarboxylic acid monoanhydride monopotassium carboxylate (1 g, 2.2 mmol), amine (11 mmol) and water (50 mL) were stirred at 0–5 °C for 4 h. After stirring the mixture at 90 °C for 2 h, potassium carbonate (25%, 12.5 mL) was added and stirred for another 1 h at 90 °C. The precipitate was collected by vacuum filtration and washed with potassium carbonate (2%). The precipitate was dissolved in KOH (3.5%, 100 mL), heated to 90 °C, kept at this temperature for 5 min and filtered while hot. After acidification with hydrochloric acid (10%), the precipitate was collected by vacuum filtration and dried in vacuum at 100 °C. Compound **3a** was purified via sublimation (−3 mbar, 300 °C). Compound **3b** was obtained in pure grade with simple purification techniques.

2.4.1. 3,4,9,10-Perylenetetracarboxylic-3,4-anhydride-9,10-imide (3a)

3a: Yield 38% (0.33 g, dark-brown powder). FT-IR (KBr, cm^{-1}): ν = 3449, 1781, 1757, 1687, 1595, 1403, 1372, 1322, 1273, 809, 735, 656. UV/vis (DMF): λ_{max} (nm) = 455, 480, 517, 559. Fluorescence (DMF): λ_{max} (nm) = 535, 575, 625. Fluorescence quantum yield ($c = 1 \times 10^{-6}$ M in $CHCl_3$, reference *N,N′*-didodecyl-3,4,9,10-perylenebis(dicarboximide) (**1a**) with $\Phi_f = 100\%$, $\lambda_{excit.} = 485$ nm) = 81%. MS: *m*/*z* (%) = 392 (M^+), 359, 341, 313, 299, 288, 271, 257, 239, 219. Anal. Calcd. for $C_{24}H_9NO_5$ (M_w, 391.3); C, 73.66; H, 2.32; N, 3.58. Found: C, 73.61; H, 2.30; N, 3.55.

2.4.2. N-(4-hydroxyphenyl)-3,4,9,10-perylenetetracarboxylic-3,4-anhydride-9,10-imide (3b)

3b: Yield 74% (0.79 g, bordeaux powder). FT-IR (KBr, cm^{-1}): ν = 3443, 3118, 1773, 1730, 1698, 1659, 1614, 1594, 1507, 1449, 1362, 1300, 1234, 1149, 1121, 1025, 938, 859, 808, 793, 758, 732, 640, 601, 571, 435. UV/vis (DMF): λ_{max} (nm) (ε) = 454 (57 000), 481 (68 000), 518 (71 000). Fluorescence (DMF): λ_{max} (nm) = 532, 565. Fluorescence quantum yield ($c = 1 \times 10^{-6}$ M in $CHCl_3$, reference *N,N′*-didodecyl-3,4,9,10-perylenebis(dicarboximide) (**1a**) with $\Phi_f = 100\%$, $\lambda_{excit.} = 485$ nm) = 25%. MS: *m*/*z* (%) = 484 (M^+), 333, 365, 393, 412, 484. Anal. Calcd. for $C_{30}H_{13}NO_6$ (M_w, 483.4); C, 74.54; H, 2.71; N, 2.90. Found: C, 74.12; H, 2.63; N, 2.75.

2.5. N-alkyl-N′-aryl-3,4,9,10-perylenebis(dicarboximide) (4a–h)

N-alkyl(aryl)-3,4,9,10-perylene tetracarboxylic monoanhydride monoimide (**3a**, **b**, 2.3 mmol), the desired primary amine (8 mmol), *m*-cresol (40 mL) and isoquinoline (4 mL) were stirred at 80 °C for 1 h. The solution was refluxed at 120 °C for 2 h, 140 °C for 2 h and 200 °C for 4 h. The warm solution was poured into 250 mL acetone. The precipitate was collected by vacuum filtration, washed with water and dried in vacuum at 100 °C. The crude product was washed with 10% NaOH in order to remove the unreacted monoimides and then extracted with corresponding alcohols in a Soxhlet apparatus for 24 h to remove high boiling solvents and unreacted amines.

2.5.1. N-dodecyl-3,4,9,10-perylenebis-(dicarboximide) (4a)

4a: Yield 90% (1.2 g, bordeaux-red powder). FT-IR (KBr, cm^{-1}): ν = 3440, 3045, 2920, 2851, 1694, 1654, 1595, 1508, 1438, 1402, 1346, 1274, 1182, 852, 810, 794, 743, 656. UV/vis (DMF): λ_{max} (nm) (ε) = 458 (40 230), 485 (65 000), 522 (87 906), 580. Fluorescence (DMF): λ_{max} (nm) = 535, 576, 623. Fluorescence quantum yield ($c = 1 \times 10^{-6}$ M in $CHCl_3$, reference *N,N′*-didodecyl-3,4,9,10-perylenebis(dicarboximide) (**1a**) with $\Phi_f = 100\%$, $\lambda_{excit.} = 485$ nm) = 80%. MS: *m*/*z* (%) = 559 (M^+), 391, 331, 299, 271, 219, 186. Anal. Calcd. for $C_{36}H_{34}N_2O_4$ (M_w, 558.7); C, 77.40; H, 6.13; N, 5.01. Found: C, 77.28; H, 6.05; N, 4.97.

2.5.2. N-(12-aminododecyl)-3,4,9,10-perylenebis-(dicarboximide) (**4b**)

4b: Yield 91% (1.2 g, red-brown powder). FT-IR (KBr, cm^{-1}): $\nu = 3420$, 2921, 2849, 1695, 1658, 1594, 1577, 1508, 1436, 1401, 1343, 1272, 1178, 1091, 853, 810, 794, 743, 654. UV/vis (DMF): λ_{max} (nm) (ε) = 456 (12 240), 487 (30 000), 523 (47 040). Fluorescence (DMF): λ_{max} (nm) = 534, 577, 623. Fluorescence quantum yield ($c = 1 \times 10^{-6}$ M in $CHCl_3$, reference *N*,*N′*-didodecyl-3,4,9,10-perylenebis(dicarboximide) (**1a**) with $\Phi_f = 100\%$, $\lambda_{excit.} = 485$ nm) = 89%. MS: *m*/*z* (%) = 574 (M^+), 507, 369, 299, 271, 201. Anal. Calcd. for $C_{36}H_{35}N_3O_4$ (M_w, 573.7); C, 75.37; H, 6.15; N, 7.32. Found: C, 75.34; H, 6.20; N, 7.14.

2.5.3. N-(octadecyl)-3,4,9,10-perylenebis-(dicarboximide) (**4c**)

4c: Yield 80% (1.2 g, red-brown powder). FT-IR (KBr, cm^{-1}): $\nu = 3450$, 3158, 3046, 2953, 2919, 2849, 1695, 1677, 1656, 1595, 1578, 1508, 1466, 1439, 1402, 1372, 1276, 1244, 1183, 1090, 882, 852, 811, 795, 743, 656, 435. UV/vis (DMF): λ_{max} (nm) (ε) = 455 (18 000), 487 (52 000), 523 (79 600), 600. Fluorescence (DMF): λ_{max} (nm) = 531, 576, 625. Fluorescence quantum yield ($c = 1 \times 10^{-6}$ M in $CHCl_3$, reference *N*,*N′*-didodecyl-3,4,9,10-perylenebis(dicarboximide) (**1a**) with $\Phi_f = 100\%$, $\lambda_{excit.} = 485$ nm) = 37%. MS: *m*/*z* (%) = 643 (M^+), 554, 391, 359, 341, 313, 267, 239. Anal. Calcd. for $C_{42}H_{46}N_2O_4$ (M_w, 642.8); C, 78.47; H, 7.21; N, 4.36. Found: C, 78.67; H, 7.19; N, 4.34.

2.5.4. N-(4-aminophenyl)-3,4,9,10-perylenebis-(dicarboximide) (**4d**)

4d: Yield 97% (1.1 g, red-brown powder). FT-IR (KBr, cm^{-1}): $\nu = 3427$, 1694, 1659, 1592, 1576, 1513, 1477, 1433, 1401, 1361, 1348, 1275, 1247, 1177, 1126, 954, 810, 742, 654. UV/vis (DMF): λ_{max} (nm) (ε) = 456 (21 500), 488 (57 000), 524 (88 200). Fluorescence (DMF): λ_{max} (nm) = 534, 576, 625. Fluorescence quantum yield ($c = 1 \times 10^{-6}$ M in $CHCl_3$, reference *N*,*N′*-didodecyl-3,4,9,10-perylenebis(dicarboximide) (**1a**) with $\Phi_f = 100\%$, $\lambda_{excit.} = 485$ nm) = 97%. Anal. Calcd. for $C_{30}H_{15}N_3O_4$ (M_w, 481.5); C, 74.84; H, 3.14; N, 8.73. Found: C, 74.83; H, 3.44; N, 8.21.

2.5.5. N-(4-chlorophenyl)-3,4,9,10-perylenebis-(dicarboximide) (**4e**)

4e: Yield 90% (1.0 g, bordeaux powder). FT-IR (KBr, cm^{-1}): $\nu = 3448$, 3065, 1701, 1670, 1592, 1577, 1492, 1432, 1402, 1358, 1346, 1272, 1246, 1176, 1090, 1018, 954, 810, 740, 654. UV/vis (DMF): λ_{max} (nm) (ε) = 458 (24 000), 489 (56 500), 526 (88 690). Fluorescence (DMF): λ_{max} (nm) = 536, 577, 624. Fluorescence quantum yield ($c = 1 \times 10^{-6}$ M in $CHCl_3$, reference *N*,*N′*-didodecyl-3,4,9,10-perylenebis(dicarboximide) (**1a**) with $\Phi_f = 100\%$, $\lambda_{excit.} = 485$ nm) = 98%. MS: *m*/*z* (%) = 501 (M^+), 411, 391, 354, 341, 313, 299, 271, 257, 235, 219. Anal. Calcd. for $C_{30}H_{13}N_2ClO_4$ (M_w, 500.9); C, 71.94; H, 2.62; N, 5.59. Found: C, 70.87; H, 2.51; N, 5.50.

2.5.6. N-(4-hydroxyphenyl)-3,4,9,10-perylenebis-(dicarboximide) (**4f**)

4f: Yield 74% (0.8 g, black powder). FT-IR (KBr, cm^{-1}): $\nu = 3413$, 1697, 1661, 1592, 1576, 1509, 1432, 1400, 1361, 1273, 1177, 954, 809, 741, 653. UV/vis (DMF): λ_{max} (nm) (ε) = 458 (25 500), 485 (36 800), 522 (40 825), 561. Fluorescence (DMF): λ_{max} (nm) = 530, 571, 619. Fluorescence quantum yield ($c = 1 \times 10^{-6}$ M in $CHCl_3$, reference *N*,*N′*-didodecyl-3,4,9,10-perylenebis(dicarboximide) (**1a**) with $\Phi_f = 100\%$, $\lambda_{excit.} = 485$ nm) = 15%. MS: *m*/*z* (%) = 483 (M^+), 391. Anal. Calcd. for $C_{30}H_{14}N_2O_5$ (M_w, 482.5); C, 74.69; H, 2.92; N, 5.81. Found: C, 74.46; H, 3.02; N, 5.50.

2.5.7. N-(12-aminododecyl)-N′-(4-hydroxyphenyl)-3,4,9,10-perylenebis(dicarboximide) (**4g**)

4g: Yield 29% (0.4 g, brown powder). FT-IR (KBr, cm^{-1}): $\nu = 3396$, 2923, 2850, 1696, 1655, 1593, 1575, 1506, 1439, 1403, 1379, 1341, 1257, 1240, 1157, 1090, 944, 852, 809, 792, 746, 630, 434. UV/vis (DMF): λ_{max} (nm) (ε) = 460 (24 000), 489 (42 400), 525 (54 320). Fluorescence (DMF): λ_{max} (nm) = 534, 574. Fluorescence quantum yield ($c = 1 \times 10^{-6}$ M in $CHCl_3$, reference *N*,*N′*-didodecyl-3,4,9,10-perylenebis(dicarboximide) (**1a**) with $\Phi_f = 100\%$, $\lambda_{excit.} = 485$ nm) = 91%. Anal. Calcd. for $C_{42}H_{39}N_3O_5$ (M_w, 665.8); C, 75.77; H, 5.90; N, 6.31. Found: C, 76.11; H, 6.08; N, 4.23.

2.5.8. N-(12-aminophenyl)-N′-(4-hydroxyphenyl)-3,4,9,10-perylenebis(dicarboximide) (**4h**)

4h: Yield 85% (1.1 g, dark-brown powder). FT-IR (KBr, cm^{-1}): $\nu = 3394$, 3195, 1699, 1656, 1593, 1575, 1514, 1432, 1402, 1359, 1294, 1254, 1177, 1122, 1007, 956, 851, 809, 796, 744, 600, 528, 489, 428. UV/vis (DMF): λ_{max} (nm) (ε) = 460 (17 000), 490 (36 230), 525 (52 570). Fluorescence (DMF): λ_{max} (nm) = 537, 570. Fluorescence quantum yield ($c = 1 \times 10^{-6}$ M in $CHCl_3$, reference *N*,*N′*-didodecyl-3,4,9,10-perylenebis(dicarboximide) (**1a**) with $\Phi_f = 100\%$, $\lambda_{excit.} = 485$ nm) = 95%. *m*/*z* (%) = 572 (M^+), 481, 373, 305, 199, 108. Anal. Calcd. for $C_{36}H_{19}N_3O_5$ (M_w, 573.6); C, 75.39; H, 3.34; N, 7.33. Found: C, 74.77; H, 3.98; N, 6.68.

3. Results and discussion

3.1. Synthesis of perylene dyes

Symmetrical perylene dyes (**1a**–**f**) were prepared by the method reported in the literature [2–6]. On the other hand, 7 new unsymmetrical perylene dyes (**4a**–**h**) were prepared according to the method described by Tröster [14]. The chemical structures of all these pigments and the synthetic pathway are illustrated in Fig. 1. The synthesis of unsymmetrical perylene dyes (**4a–h**) was accomplished in three steps. Starting from perylene-3,4,9,10-tetracarboxylic acid dianhydride, perylene-3,4,9,10-tetracarboxylic acid monoanhydride monopotassium carboxylate (**2**) was first prepared, followed by the preparation of *N*-alkyl(aryl)-3,4,9,10-perylene tetracarboxylic monoanhydride monoimide (**3a**, **b**), and finally *N*-alkyl-*N'*-aryl-3,4,9,10-perylenebis(dicarboximide) (**4a–h**). The amines used at the third step and in the synthesis of compounds (**1a–f**) were the same in order to enable direct comparison of properties. Due to the necessity of an aqueous medium at the second step, the water soluble primary amines gave better yields of **3**.

Purification of **4** was relatively straightforward because of the widely different solubilities of **2**, **3** and **4** in cold and hot KOH solutions. Compound **2** could be easily dissolved in cold or hot KOH solution. Compound **3** was soluble only in hot KOH solution. Compound **4** was insoluble in hot or cold KOH solution.

The structure of the synthesized symmetrical perylene dyes (**1a–f**) was characterized by elemental analysis, FT-IR, MS and ^{1}H NMR spectral data. However, NMR measurement of unsymmetrical perylene dyes (**4a–h**) could not be taken due to the poor solubility of the compounds in solvents.

The color of the compounds in the solid state varied widely depending on the substituents. Characteristic imide bands were observed in all the IR spectra. Mass spectra for most of the compounds showed the corresponding molecular ion peak. But mass spectra for **4d** and **4g** were not obtained because of their low volatility.

3.2. Spectral characteristics of symmetrical and unsymmetrical perylene dyes

Solubility of all the unsymmetrical perylene dyes is very poor compared to their symmetrical ones. The UV/vis absorption spectra of the symmetrical (**1a–f**) and unsymmetrical (**4a–h**) perylene diimides are nearly identical except **1d**. Large red shift is observed for the compound **1d** (14 nm) due to the intermolecular π-stacking interactions in acetone. Further, **1c**, **1d**, **1f**, **4a**, **4c** and **4f** exhibit weak and broad absorptions at longer wavelengths in the visible region, 500–700 nm even at 10^{-5} M concentration (Fig. 2, Table 1). Aroca has informed a similar broad band on the visible absorption spectrum of *N*-(octadecyl)-3,4,9,10-perylenebis(dicarboximide) (**4c**) at 590 nm (3.58×10^{-5} M). He assumed that the reason for the new band was the formation of aggregates in solution [19].The new absorption bands observed on absorption spectra of **1c**, **1d**, **1f**, **4a**, **4c**

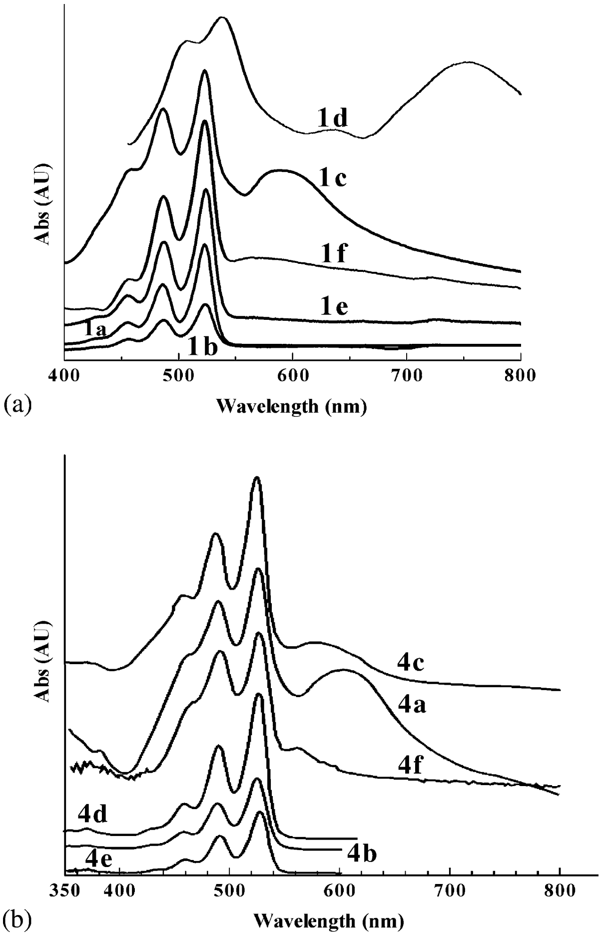

Fig. 2. The absorption spectra of **1a–c**, **1e**, **1f** (a) and **4a–f** (b) in DMF. The absorption spectra of **1d** in acetone (10^{-5} M).

Table 1
The UV–vis absorption and fluorescence maximum wavelengths and extinction coefficients ε_{max} (l mol^{-1} cm^{-1})

No.	UV–vis[a] (nm)	FL[b] (nm)
1a	454(18 580), 487(52 850), 523(87 630)	536, 574, 628
1b	454, 487, 523	537, 578, 630
1c	458(18 580), 489(52 850), 525(86 100), 582	535, 576, 624
1d[c]	506(52 000), 537(80 064), 633, 754	537, 578, 626
1e	458(37 000), 489(65 000), 525(90 156)	534, 577, 624
1f	454(14 450), 486(28 500), 522(40 240), 564	534, 578, 621
4a	458(40 230), 485(65 000), 522(87 906), 580	535, 576, 623
4b	456(12 240), 487(30 000), 523(47 040)	534, 577, 623
4c	455(18 000), 487(52 000), 523(79 600), 600	531, 576, 625
4d	456(21 500), 488(57 000), 524(88 200)	534, 576, 625
4e	458(24 000), 489(56 500), 526(88 690)	536, 577, 624
4f	458(25 500), 485(36 800), 522(40 825), 561	530, 571, 619
4g	460(24 000),489(42 400), 525(54 320)	534, 574
4h	460(17 000), 490(36 230), 525(52 570)	537, 570

[a] UV–vis spectra were obtained at a concentration of 10^{-5} M in DMF.

[b] Fluorescence spectra in DMF, $\lambda_{excit.} = 485$ nm.

[c] In acetone.

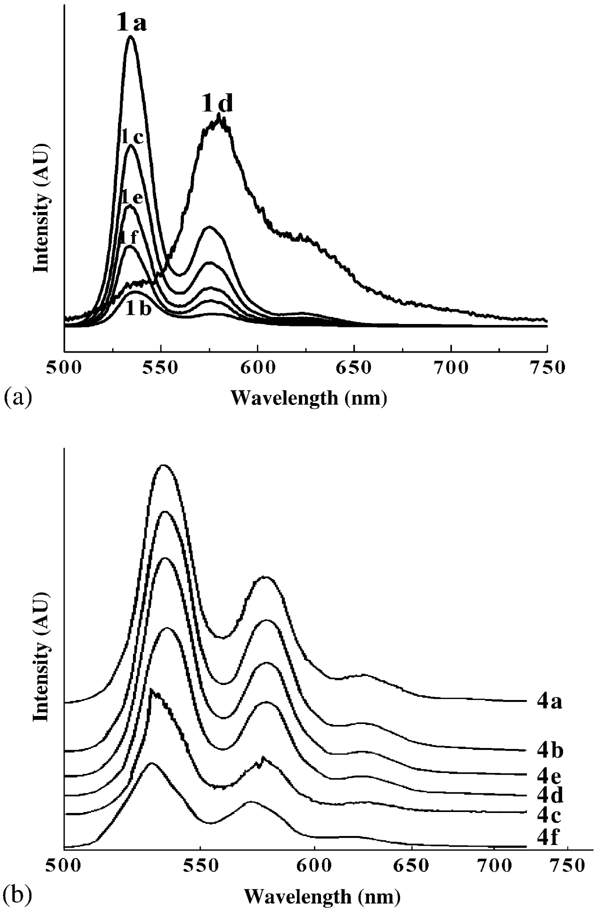

Fig. 3. The fluorescence spectra of **1a–f** (a) and **4a–f** (b) in DMF.

and **4f** are attributed to aggregation and disappear upon filtration of the solutions through a 0.2 μm SPR microfilter. The spectral data of the unaggregated form are very similar to that of solutions.

The emission spectra of all the compounds were taken at $\lambda_{\text{excit.}} = 485$ nm with *N*,*N*′-didodecyl-3,4,9,10-perylenebis(dicarboximide) (**1a**) as the standard. The fluorescence spectra of the compounds, (**1a–f**) and (**4a–f**) were very similar as well as their absorbance spectra (Figs. 2–4 and Table 1).

On the other hand, the emission spectra of **1d** in DMF show characteristically broad excimer-like emission band at 578 nm (Fig. 3a). Notably, the excimer-like emission and the low fluorescence rate constant in DMF suggest the formation of ground state complexes probably due to intermolecular π-stacking of the compound (Fig. 3a, Table 2) in solution. As expected the fluorescence quantum yields of most symmetrical perylene dyes are very high. Meanwhile, the fluorescence quantum yields are reduced to a different extent for the compounds **1d** and **1f** possibly due to the aggregation (Table 2) in the liquid state. Recently, we reported the synthesis and photophysical properties of, *N*,*N*′-bis(4-cyanophenyl)-3,4,9,10-perylenebis(dicarboximide) (CN-PDI). On the absorption spectrum of the compound we observed a new broad band at 579 nm even at 10^{-5} M and the fluorescence quantum yield was measured as 0.136 at $\lambda_{\text{excit.}} = 485$ nm with *N*,*N*′-didodecyl-3,4,9,10-perylenebis(dicarboximide) (**1a**) as the standard. The low fluorescence quantum yield and the new band were attributed to molecular aggregation. The low fluorescence quantum yield of **1d**, **1f**, **4c** and **4f** is in good correlation with the literature data of CN-PDI [21].

Interestingly, the similarity in the solution spectra of perylene dyes despite their differing color at solid state supported that the substituents are not involved in the chromophore (Figs. 2–4).

Maximum absorption wavelength ($\lambda_{\max}$ in nm, DMF), fluorescence quantum yields (Φ_f, DMF), radiative lifetimes τ_0 (ns), fluorescence lifetimes τ_f (ns), fluorescence rate constants k_f ($10^8 s^{-1}$), and singlet energies E_s (kcal mol^{-1}) data of all the compounds in DMF, are given in Table 2. Fluorescence lifetimes of the compounds were measured in argon-saturated solutions.

The theoretical radiative lifetimes τ_0 were calculated according to the formula: $\tau_0 = 3.5 \times 10^8/\nu_{\max}^2\,\varepsilon_{\max}\,\Delta\nu_{1/2}$, where $\nu_{\max}$ stands for the wavenumber in cm^{-1}, $\varepsilon_{\max}$ for the molar extinction coefficient at the selected absorption wavelength and $\Delta\nu_{1/2}$ indicates the half-width of the selected absorption in units of cm^{-1} [17]. Fluorescence lifetimes were calculated from $\tau_f = \tau_0\,\Phi_f$ and the rates of fluorescence from $k_f = 1/\tau_0$ (Table 2). The technique of time correlated single photon counting was used to record fluorescence lifetimes of the compounds. The

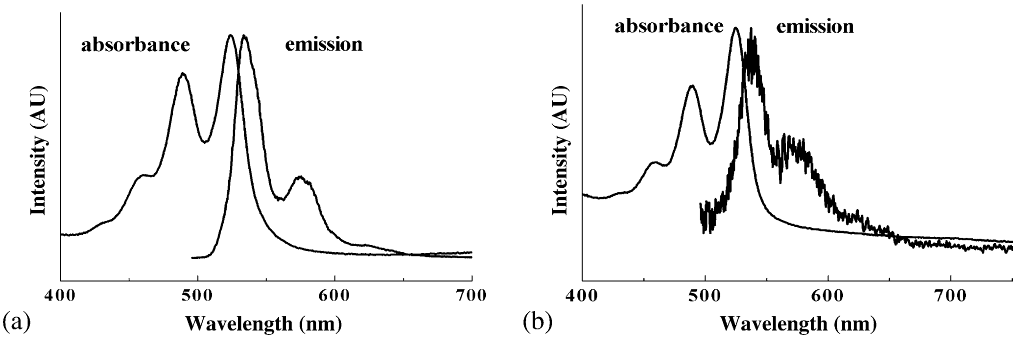

Fig. 4. The absorbance and fluorescence ($\lambda_{\text{excit.}} = 485$ nm) spectra of **4g** (a) and **4h** (b) in DMF.

Table 2
Maximum absorption wavelengths λ_{max} (nm), extinction coefficients ε_{max} (l mol^{-1} cm^{-1}), fluorescence quantum yields Φ_f ($\lambda_{excit.}$ = 485 nm), radiative lifetimes τ_0 (ns), fluorescence lifetimes τ_f (ns), fluorescence rate constants k_f (10^8 s^{-1}) and singlet energy E_s (kcal mol^{-1}) data of **1a–f** and **4a–h** in DMF

	λ_{max}	ε_{max}	Φ_f	τ_0	τ_f[a]	k_f	E_s
1a	523	87630	1	9	9 (4.1)	1.1	54.7
1b	523	–	0.83	–	– (4.1)	–	54.7
1c	525	86100	0.80	9.2	7.4 (3.8)	1.4	54.5
1d	537	80064	0.20	16	3.2 (3.8)	3.1	53.3
1e	525	90156	0.84	8.8	7 (4)	1.5	54.4
1f	522	40240	0.20	24.7	4.9 (3.9)	2.0	54.8
4a	522	87906	0.80	8.9	6.8 (3)	1.5	54.8
4b	523	47040	0.89	16.7	8.2 (2.7)	1.2	54.7
4c	523	79600	0.37	13.2	4.9 (3)	2.0	54.7
4d	524	88200	0.97	8.9	8.6 (2.9)	1.2	54.9
4e	526	88690	0.98	8.9	8.7 (3.1)	1.2	54.4
4f	522	40825	0.15	33.3	5 (2.8)	2	54.8
4g	525	54320	0.91	30	3 (2.7)	3.3	54.5
4h	525	52570	0.95	27	2.7 (3.1)	3.7	54.5

[a] Experimental values are given in parentheses.

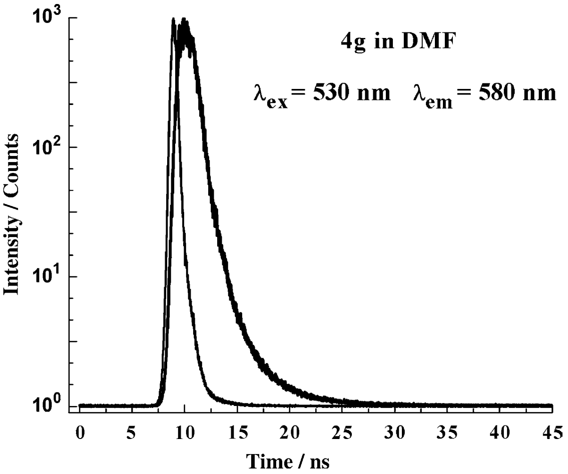

Fig. 5. Fluorescence decay curve of 10^{-5} M **4g** ($\lambda_{excit.}$ = 530 nm and λ_{em} = 580 nm) in DMF.

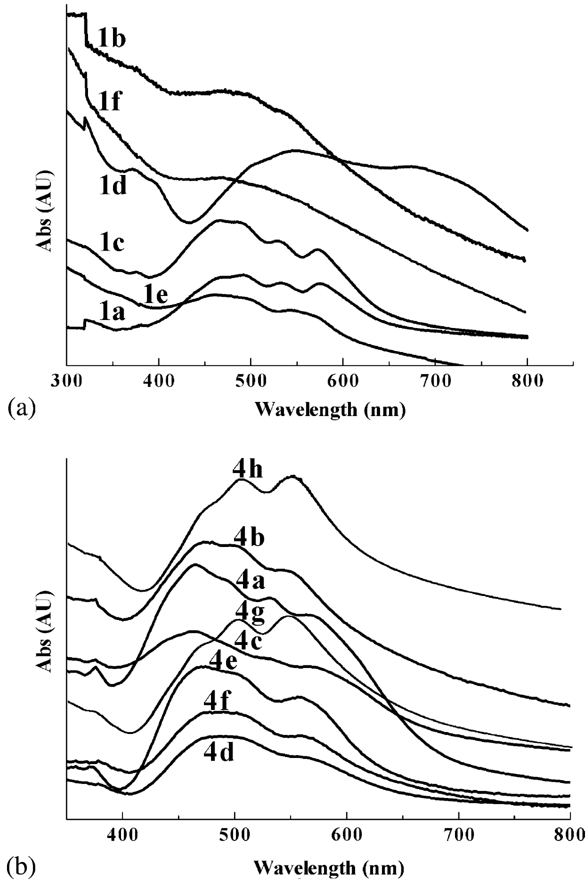

Fig. 6. Solid-state UV/vis absorption spectra of **1a–f** (a) and **4a–h** (b).

decay curves were multi-exponential and analysed by using the standard method of iterative reconvolution and non-linear least square fitting method (Fig. 5). The quality of calculated fits was judged using statistical parameters, the reduced χ^2 value and the residual data. As can be seen from Table 2, the calculated and measured fluorescence lifetimes of all the symmetrical and unsymmetrical perylene dyes are very similar.

The different intermolecular interactions in solid state seem to change the color variously. The shapes of the absorption spectra of all the perylene dyes in solution and in the solid state show drastic differences, in view of wavelength range (absorption up to 700 nm) and peak positions (Fig. 6). This spectral change is attributed to intermolecular π interaction in the solid state. Notably, the peak positions in solid state absorption spectra of the symmetrical and unsymmetrical perylene dyes were not similar (Fig. 6). This is attributed to the different intermolecular interactions via unsymmetrical substituents.

3.3. Thermal stability

Thermal analyses of the compounds were studied by thermogravimetry (TGA) (Fig. 7) and differential scanning calorimetry (DSC) (Fig. 8). The pressure of a higher alkyl chain in the symmetrical and unsymmetrical perylene dyes appeared to lower the decomposition temperature. Further, the degradative temperature of the aryl or alkyl substituted symmetrical dyes was higher than that in unsymmetrical ones (Fig. 7, **1a–4a**: 453–339 °C, **1b–4b**: 412–304 °C, **1c–4c**: 314–311 °C, **1d–4d**: 543–434 °C, **1e–4e**: 551–500 °C, **1f–4f**: 622–552 °C). The higher degradation temperature for the *N*-aryl substituted compounds (**1d**: 543 °C, **1e**: 551 °C, **1f**: 622 °C, **4d**: 434 °C, **4e**: 500 °C, **4f**: 552 °C, **4g**: 445 °C, **4h**: 500 °C) as compared with the *N*-alkyl (**1a**: 453 °C, **1b**: 412 °C, **1c**: 314 °C, **4a**: 339 °C, **4b**: 304 °C, **4c**: 311 °C) compounds, indicates that the degradation of an aryl group occurs at a higher temperature (Fig. 7).

The symmetrical and unsymmetrical dyes, exhibit no glass transition temperature during DSC runs (1st and

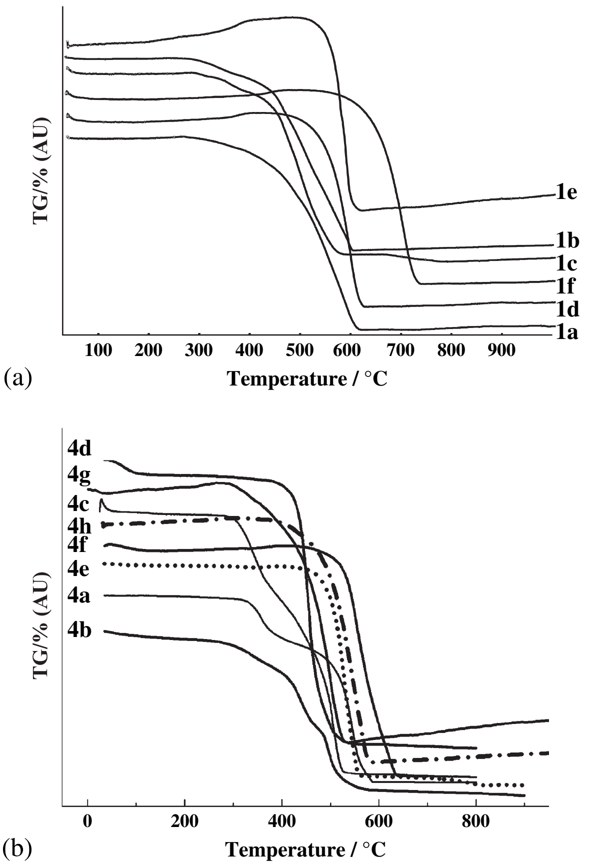

Fig. 7. Thermogravimetric analysis curves of **1a–f** (a) and **4a–h** (b) at a heating rate of 5 K/min in oxygen.

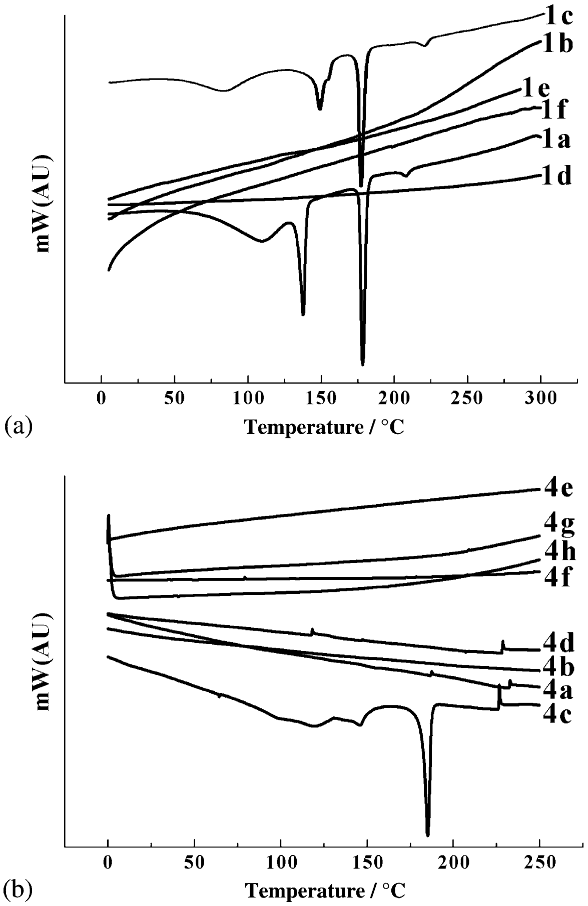

Fig. 8. DSC thermograms of **1a–f** (a) and **4a–h** (b).

2nd heating) up to 300 °C. Among all the compounds, only the compounds **1a**, **1c** and **4c** show a melting point. The DSC thermogram of compound **1a** (Fig. 8a) exhibits three endothermic peaks at 110.33 (Δ*H*: −133.01 mJ), 137.67 (Δ*H*: −60.79 mJ) and 178.33 °C (Δ*H*: −10.54 mJ) during the 1st and 2nd heating. The first two peaks indicate a transition and the third is a typical melting peak. Also, the DSC thermogram of compound **1c** (Fig. 8a) exhibits three endothermic peaks at 83.17 (Δ*H*: −60.67 mJ), 147.83 (Δ*H*: −56.27 mJ) and 175.83 °C (Δ*H*: −60.72 mJ) during the 1st and 2nd heating. The first two peaks show a transition and the third is the melting peak. Finally, the DSC thermogram of compound **4c** (Fig. 8b) shows three endothermic peaks at 118.82, 149.00 (Δ*H*: −67.46 mJ) and 187.00 °C (Δ*H*: −34.57 mJ) during the 1st and 2nd heating. The first two peaks belong to a transition and the third is the melting peak.

3.4. Electrochemistry of symmetrical and unsymmetrical perylene dyes

All the compounds display reduction processes in their cyclic (CV) and square-wave voltammetries (Fig. 9). Table 3 summarizes the electrochemical parameters obtained [22,23]. Low solubility of unsymmetrical dyes has caused difficulties for the measurements of cyclic voltammograms.

The electrochemistry of these compounds was investigated by square-wave voltammetry in butyronitrile. Compound **1b** has poor solubility in DMF and DMSO. Unfortunately, these solvents are not useful for voltammetry measurements of these compounds because these solvents are reduced in the same range. Due to this reason the voltammogram of **1b** could not be recorded in solution.

The LUMO energies of all the compounds were calculated from cyclic and square-wave voltammograms (Table 3). These values were calculated based on the value of 4.8 eV for Fc with respect to zero vacuum level [23,24].

The first reduction potentials and LUMO values for all of the compared symmetrical and unsymmetrical perylene dyes are nearly identical. The difference on the other reduction steps is attributed to substituents effect. In the cyclic voltammetry, the corresponding cathodic and anodic peak separation value for each reversible reduction step is approximately 60–70 mV at a scan rate of 100 mV s^{-1} as expected for a fast reversible single electron transfer.

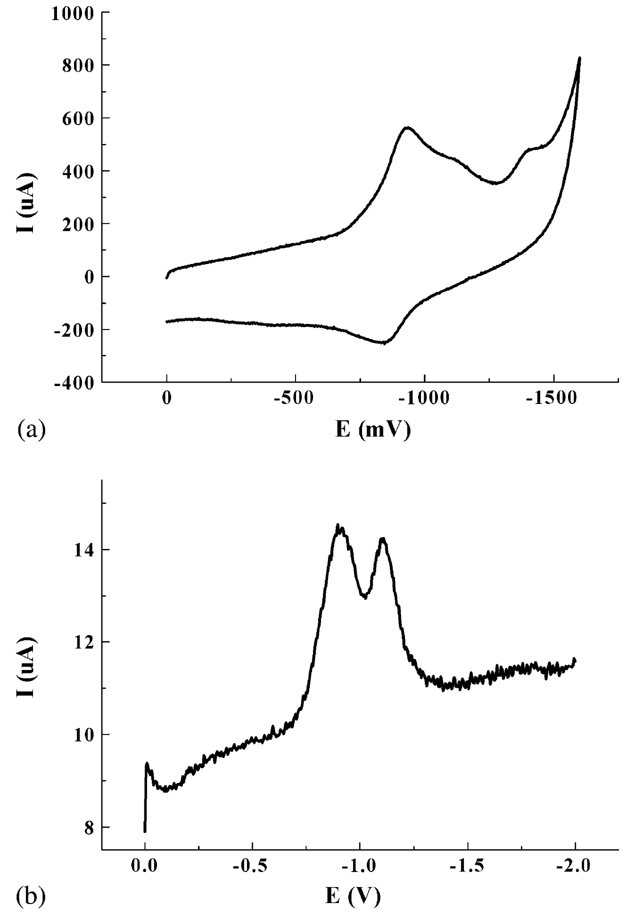

Fig. 9. Cyclic and square-wave voltammograms of compounds **1e** (a) (in butyronitrile/supporting electrolyte: TBAPF6, scan rate: 100 mV s^{-1}) and **4e** (b) (in butyronitrile/supporting electrolyte: TBAPF6, frequency: 60 Hz) at 25 °C.

Table 3
Cyclic[a,b] and square-wave voltammetry[a,c] data and LUMO values of compounds **1a–f** and **4a–h**

	$E_{\mathrm{Red1-Red3}}$ vs. Ag/AgNO$_3$ (V)	E_{Fc} vs. Ag/AgNO$_3$ (V)	$E_{1/2}$ vs. Fc (V)	LUMO (eV)
1a	−0.81 −0.95	0.25	−1.06 −1.2	−3.74
1c	−0.90	0.26	−1.16	−3.64
1d	−1.01 −1.28 −1.46	0.16	−1.17 −1.44 −1.62	−3.63
1e	−0.90 −1.14 −1.43	0.25	−1.15 −1.39 −1.68	−3.65
1f	−0.91 −1.26	0.16	−1.07 −1.42	−3.73
4a	−0.96 −1.24	0.15	−1.11 −1.39	−3.69
4b	−0.95 −1.26	0.18	−1.13 −1.44	−3.67
4c	−0.95 −1.23	0.16	−1.11 −1.39	−3.69
4d	−0.95 −1.11	0.15	−1.11 −1.26	−3.69
4e	−0.91 −1.10	0.14	−1.05 −1.24	−3.75
4f	−0.94 −1.16	0.15	−1.09 −1.31	−3.71
4g	−1.08	0.16	−1.24	−3.56
4h	−1.00	0.18	−1.18	−3.62

[a] Supporting electrolyte, 0.1 M tetrabutylammonium hexafluorophosphate (TBAPF6).
[b] Scan rate of 100 mV s^{-1}.
[c] Frequency of 60 Hz. [**1a–f**] = 1 × 10^{-3} M, [**4a–h**] = 1 × 10^{-4} M.

4. Conclusion

The synthesis of new unsymmetrical perylene diimides has been achieved (**4a–h**). For comparison, the symmetrical derivatives of all the compounds have been synthesized by the method previously reported (**1a–f**). We have established their photophysical, thermochemical and electrochemical properties. The results were: (i) the solubility of all the unsymmetrical perylene dyes is very poor compared to their symmetrical ones. (ii) The UV/vis absorption spectra of all the compounds in solutions are almost similar. Meanwhile, the solid state UV spectra are drastically different. (iii) The degradative temperatures of the aryl or alkyl substituted symmetrical dyes are higher than that in unsymmetrical ones and most of the unsymmetrical perylene dyes do not melt until 250 °C. (iv) Fluorescence intensity decreases in some symmetrical and unsymmetrical dyes probably due to the aggregation. (v) The lifetimes for the compounds (**4a–h**), monitored at 580 nm, show no significant deviation from that of the compounds (**1a–f**). (vi) Little difference is observed between the two first reduction potentials and singlet-state energies of all the compounds. (vii) The color, solubility, aggregation, thermal stability, melting point and fluorescence quantum yields are effected from substituents.

Acknowledgments

We gratefully acknowledge financial support by the Scientific Research Council of Turkey under contract no.TBAG-1707.

References

[1] Langhals H. Heterocycles 1995;40:477–500.
[2] Demmig S, Langhals H. Chem Ber 1988;121:225–30.
[3] Icli S, Icil H. Spectrosc Lett 1996;29(7):1253–7.
[4] Icil H, Arslan E. Spectrosc Lett 2001;34(3):355–63.
[5] Icil H, Uzun D, Arslan E. Spectrosc Lett 2001;34(5):605–14.
[6] Icil H, Icli S. Spectrosc Lett 1995;28(4):595–601.
[7] Meissner D, Rostalski J. Synth Met 2001;121:1551–2.
[8] Rostalski J, Meissner D. Sol Energy Mater Sol Cells 2000; 63:37–47.
[9] El-Daly SA, Fayed TA. J Photochem Photobiol A Chem 2000; 137:15–9.

[10] Nagao Y, Ishikawa N, Tanabe Y, Misono T. Chem Lett 1979;115–51.
[11] Nagao Y, Misono T. Bull Chem Soc Jpn 1981;54:1269–70.
[12] Nagao Y, Misono T. Bull Chem Soc Jpn 1981;54:1191–4.
[13] Nagao Y, Misono T. Dyes Pigments 1984;5:171–88.
[14] Tröster H. Dyes Pigments 1983;4:171–7.
[15] Langhals H, Ismael R, Yuruk O. Tetrahedron 2000;56:5435–41.
[16] Kaiser H, Lindner J, Langhals H. Chem Ber 1991;124:529–35.
[17] Langhals H, Feiler L. Liebigs Ann 1996;1587–91.
[18] Gonzalez JD, Aroca R, Nagao Y, Desaja JA. Spectrochim Acta Part A 1997;53:173–81.
[19] Sallack J, Maiti AK, Aroca R, Menendez JR. J Mol Struct 1997;410–411:217–21.
[20] Zhavnerko GK, Kuchuk TA, Agabekov VE, Gallyamov MO, Yaminskii IV. Russ J Phys Chem 1999;73:1111–4.
[21] Uzun D, Ozser ME, Yuney K, Icil H, Demuth M. J Photochem Photobiol A 2003;156:45–54.
[22] Turro NJ. Molecular photochemistry. London: Benjamin; 1965.
[23] Koepp HM, Wendt H, Strehlow H. Z Electrochem 1960; 64:483–91.
[24] Bredas JL, Silbey R, Bourdreaux DS, Chance RR. J Am Chem Soc 1983;105:6555–9.